# ADAPTATION OF ROADS TO ALS DATA BY MEANS OF NETWORK SNAKES

J. Goepfert, F. Rottensteiner

Institute of Photogrammetry and GeoInformation, Leibniz University of Hannover
(goepfert, rottensteiner)@ipi.uni-hannover.de

**Commission III, WG III/2**

**KEY WORDS:** snakes, networks, vector data, roads, ALS, intensity, topology, consistency

**ABSTRACT:**

In the Authoritative Topographic Cartographic Information System (ATKIS®), which is the main public topographic data base in Germany, the heights and the 2D positions of objects such as roads are stored separately in the digital terrain model (DTM) and digital landscape model (DLM). However, for many applications a combined visualization and processing of these two data sets is useful, leading to the demand for a 3D representation of the objects. For this purpose an integration of the height and position is essential. However, discrepancies exist between the DLM and the DTM due to different kinds of acquisition, processing, and modeling. This inconsistency has to be solved within the integration algorithm. Airborne Laserscanning (ALS) is used to acquire the height information for the DTM. Therefore, intensity values of the ALS echoes, which contain the reflectance properties of the illuminated objects, as well as object heights can be exploited in addition to the terrain height. However, the ALS data contain the information related to the DLM-objects only implicitly. Usually, features, for example edges or distinctive points, have to be extracted which can be connected to DLM-objects to realize the integration process. In this paper the matching of the data sets is realized by network snakes which are able to use the implicit ALS information about the position of the DLM-objects without the feature extraction step. The initialization of the contour with the vector data enables the use of ALS data as image energy for an iterative optimization process. Examples are given which apply the concept of network-snakes for the adaptation of a road network to ALS data taking advantage of the prior known topology.

## 1. INTRODUCTION

### 1.1 Motivation

The German Authoritative Topographic Cartographic Information System (ATKIS®) basically consists of the digital landscape model (DLM) and the digital terrain model (DTM). These two components are extensively used for applications with relation to the topography of the earth in different fields of administration, research and industry. The DLM describes the objects on the earth's surface using 2D vector data and additional attributes, whereas the DTM is a continuous 2.5D representation of the surface modeled by terrain points in a regular grid or triangulated irregular network (TIN).

3D modeling of the topographic objects is often required for applications such as planning of infrastructure or flood risk modeling. For this purpose an integration of the 2D vector data and the height information is necessary. However, discrepancies exist between the DLM and the DTM due to different methods of acquisition, processing, and modeling (Figure 1). Examples for such inconsistencies are bodies of standing water having physically impossible height variations or streets with invalid height gradients. As a consequence, integration without matching the data sets leads to semantically incorrect results. Thus, the two data sets have to be adapted for accurate combined visualization and processing.

The DTM used in the paper is collected by the surveying authority of Schleswig-Holstein by Airborne Laserscanning (ALS). ALS delivers a digital surface model (DSM), from which the DTM is generated by filtering methods. ALS data also contain the intensity of the reflected signal, which can be exploited in addition to the height data. The DSM also contains information about objects situated on the terrain (e.g. buildings or trees). Vector data adapted to the DSM and the ALS intensity data should also match the DTM. We are mainly interested in roads, which typically have an accuracy of 3-5 m in ATKIS, with local deviations that may reach 10 m. It is thus the goal of this paper to present an algorithm for improving 2D road vector data using the DSM and intensity data generated from ALS.

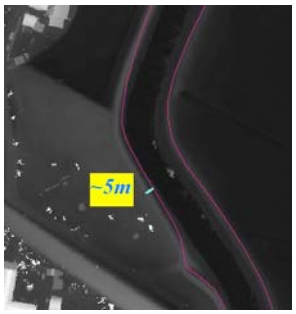


Figure 1. Inconsistency between 2D vector data and the DSM

In order to improve road data base using ALS data, features extracted in the DSM could be matched with DLM objects. In this paper, a top-down method based on active contours is proposed. Whereas the contour is initialized by the vector data, the DSM or related products act as the image energy, which attracts the contour to salient features.

### 1.2 Related Work

The integration of a DTM with 2D GIS data has been analysed for several years. Initial methods such as height attributing of

object points or adding interactive DTM interfaces to GIS software (Weibel, 1993) do not realize a real merging process of the two data sets. Later, some authors (Pilouk 1996; Lenk 2001) investigate the incorporation of the 2D geometry of the vector objects into a DTM modelled by a TIN. However, these algorithms do not consider the inconsistencies between the vector data and the DTM resulting in a semantic incorrectness of the merged data set. Rousseaux & Bonin (2003) model 2D linear objects such as roads and dikes as 2.5D surfaces by using attributes of the GIS data base and the height information of the DTM with the goal of generating an improved DTM. They use slopes and regularization constraints to check the semantic correctness of the objects, but they do not adapt the objects if this check fails, the correctness is not established. Koch (2006) extends the integration methods based on TIN structures by a least squares adjustment using equality and inequality constraints in order to incorporate the semantics of the objects. However, this approach is very sensitive to the definition of the weights if the position and the height observations are corrected simultaneously. Furthermore, the implicit information about the vector objects in the DTM such as structure lines at road embankments is not considered. In this paper these deficits are tackled by using the ALS data as image energy for active contours in order to correct the position of the objects considering their height information.

Active contour models (Kass et al., 1988) combine the feature extraction and geometric object representation in image analysis. Two realisations of this model are distinguished in the literature. Whereas the parametric active contour (Kass et al., 1988; Blake & Isard, 1998), also called snake, is an explicit representation of the contour in its parametric form, the geometric active contour (Malladi et al., 1995; Caselles et al. 1997) describes the contour as a zero level line of a level set function. The main advantage of the level set approach arises from its flexible topology. In contrast the parametric method has to be extended in order to enable splitting and merging of entities (McInerny & Terzopoulos, 1995). For the goals of this paper the topology of the given road network has to be preserved. For that reason the network-snake algorithm of Butenuth (2008) is used with new definitions of the image energy functions. The basic concept of snakes is widely used in image and point cloud analysis as well as GIS applications. For example, Burghardt & Meier (1997) suggest an active contour algorithm for feature displacement in automated map generalisation. Cohen & Cohen (1993) introduce a finite elements method for 3D deformable surface models and Kerschner (2001) applies a twin snake model for seam line detection in orthoimage mosaicking. Borkowski (2004) shows the capabilities of Snakes for break line detection in the context of surface modelling. Laptev et al. (2001) extract roads using a combined scale space and snake strategy.

In order to extract roads from ALS data, Rieger et al. (1999) propose twin snakes to model roads as parallel edges. This integration of model based knowledge stabilises the extraction and is able to bridge gaps in the structure lines in the vicinity of roads, which are often not continuous in nature. Road extraction can also be improved by fusing ALS and image data, e.g. (Zhu et al., 2004), as well as GIS data (Oude Elberink & Vosselman, 2006). The ALS intensity values, assumed to be a by-product a few years ago, can also be exploited in the extraction process. Roads have usually small intensity values and are well represented and distinguishable from their neighbourhood by this feature, along with the fact that they are situated on the DTM. This fact is used by Alharthy & Bethel (2003) and Clode et al. (2007) for road extraction.

## 2. METHOD

### 2.1 General Work Flow

In this paper a top-down method based on active contours is proposed in order to adapt road networks from ATKIS data base to ALS data. The topology of the object parts is incorporated in the algorithm by the concept of network snakes. Thus, contour parts with weak evidence in the image energy can be supported by others in the optimization process. The initialization and therefore the internal energy are obtained by the vector data modeled by spline terms (cf. section 2.2), while the ALS information defines the new image energy forcing the snake to salient features (cf. section 2.3). However, ATKIS vector data are usually stored in polylines without considering the topology of the network. Therefore the topology is reconstructed by searching for nodes which occur multiple times. After defining and weighting the different terms of internal and image energies the iterative optimisation process is started modifying the position of the network snake. The change of the position of the contour in the current iteration is used to determine the convergence of the algorithm. Afterwards, the new position of the contour should match the corresponding features for the road network in the ALS data.

### 2.2 Snakes and network snakes

In the general idea of snakes the position of the contour in an image is determined in an iterative energy optimisation process. An initialisation of the contour is required. Three energy terms (Equation 1) are introduced by Kass et al. (1988). The internal energy defines the elasticity and rigidity of the curve. The image energy should represent the features of the object of interest in an optimal manner in order to attract the contour step by step to the desired position. Additional terms (constraint energy) can be integrated in the energy functional forcing the contour to fulfil predefined external constraints.

$$E^*_{snake} = \int_0^1 E_{Snake}(v(s))ds$$

$$= \int_0^1 (E_{\text{int}}(v(s)) + E_{image}(v(s)) + E_{con}(v(s)))\,ds \qquad (1)$$

where $v(s) = (x(s), y(s))$ is the parametric curve with arc length s.

At first a closer look at the internal energy is taken. Motivated by the definition of splines this term can be written as:

$$E_{\text{int}}(v(s)) = \frac{\alpha(s)\cdot|v_s(s)|^2 + \beta(s)\cdot|v_{ss}(s)|^2}{2} \qquad (2)$$

where $v_s$, $v_{ss}$ = derivatives of v with respect to s
$\alpha$, $\beta$ = weights

The first order term, weighted by α, is responsible for the elasticity of the curve. Due to the arc length minimizing effect high values of α result in very straight curves. The second order term, weighted by β, forces the snake to act like a thin plate and determines the rigidity of the curve. High values of β cause a

smooth curve while contour parts with a small β are able to model the behaviour of corners.
The image energy (cf. section 2.3) can be simply defined using the image intensity itself, in order to attract the contour to dark or in case of a negative sign to bright lines. If the desired objects are represented by image edges, functions of the magnitudes of the gradient image are able to describe the image energy in a sufficient manner. Other authors use terms derived from a distance map related to the closest edge pixel (Cohen & Cohen, 1993) or the gradient vector flow (GVF) (Xu & Prince, 1997) for an improved representation of the image energy.

In order to obtain the optimal position of the snake in the image, the energy functional in Equation 1 has to be minimised. For the sake of simplicity the sum of image and constraint energy is set to external energy $E_{ext}$ and the weight parameters α and β are kept constant along the entire contour. In that case the minimisation of the functional results in the two independent Euler equations (for x and y):

$$\frac{\delta E_{ext}(v(s))}{\delta v(s)} + \alpha \cdot v_{ss}(s) + \beta \cdot v_{ssss}(s) = 0 \tag{3}$$

The derivatives can not be calculated analytically. Thus, they are approximated in the following by means of finite differences. The transfer to the discrete formulation of the energy functional facilitates the variation of the weights along the contour. With the substitution $f_v(v_i) = \delta E_{ext} / \delta v_i$ the Euler equations can be rewritten:

$$\begin{aligned} &\alpha_i \cdot (v_i - v_{i-1}) - \alpha_{i+1} \cdot (v_{i+1} - v_i) \\ &+ \beta_{i-1} \cdot (v_{i-2} - 2v_{i-1} + v_i) - \beta_i \cdot (v_{i-1} - 2v_i + v_{i+1}) \\ &+ \beta_{i+1} \cdot (v_i - 2v_{i+1} + v_{i+2}) + (f_v(v_i)) = 0 \end{aligned} \tag{4}$$

In the basic formulation all finite differences can be calculated, if v(s) represents a closed contour with v(0) = v(n). Equation (4) in matrix form reads:

$$Av + f_v(v_i) = 0 \tag{5}$$

A is a pentadiagonal banded matrix, except for the entries concerning the connection of the first and the last point of a closed contour. In order to solve Equation 5 the right hand side is set equal to the product of a defined step size and the negative time derivatives of the left side. By assuming that the derivatives of the external energy $f_v(i)$ are constant during a time step, an explicit Euler step regarding the image energy is obtained. The internal energy completely determined by the banded matrix results in an implicit Euler step if the time derivative is calculated at time t rather than t-1. Following these considerations the problem is now specified by:

$$Av_t + f_v(v_{t-1}) = -\gamma(v_t - v_{t-1}) \tag{6}$$

where γ is the step size. The time derivative vanishes at equilibrium and Equation 6 corresponds to Equation 5. By means of matrix inversion the final solution results in:

$$v_t = (A + \gamma \cdot I)^{-1} \cdot (\gamma \cdot v_{t-1} - f_v(v_{t-1})) \tag{7}$$

This basic formulation of the energy minimisation of the snake is valid for closed contours. However, Butenuth (2008) extends this concept to networks of contours taking nodes with higher degree into account. In Figure 2 an example of a road network containing nodes of different degrees is given to illustrate the task. The extended topology of the net requires a few changes in the definition of the internal energy due to the lack of some finite differences. Because the nodes $v_{i+1}$ (Equation 4) are not available related to end nodes and nodes of higher degree (>2), the first term of the internal energy defining the elasticity is not defined and, thus, not considered. The existing differences are used for the definition of the second term which controls the curvature and is weighted by β. For the node $v_n = v_a = v_b = v_c$ with a degree of three the energy is defined as:

$$\begin{aligned} &\beta \cdot (v_{a_n} - v_{a_{n-1}}) - \beta \cdot (v_{a_{n-1}} - v_{a_{n-2}}) + f_{v_a}(v_a) = 0 \\ &\beta \cdot (v_{b_n} - v_{b_{n-1}}) - \beta \cdot (v_{b_{n-1}} - v_{b_{n-2}}) + f_{v_b}(v_b) = 0 \\ &\beta \cdot (v_{c_n} - v_{c_{n-1}}) - \beta \cdot (v_{c_{n-1}} - v_{c_{n-2}}) + f_{v_c}(v_c) = 0 \end{aligned} \tag{8}$$

The three contour parts intersect each other in the common point and due to the mentioned definition of the internal energy the shape of each part is controlled separately except for the intersection point, of course. Thus, the initial topology of the network is taken into account and furthermore can be exploited during the energy minimisation process. Subsequently, the matrix A has to be reorganised separating contour parts which are not connected as well as adding entries for new relations between adjacent nodes. For end nodes and nodes with higher degree (>3) a similar definition of the internal energy can be applied by adding or excluding equations in (8) related to the degree of the considered node point.

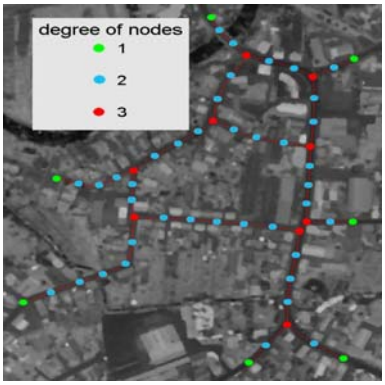


Figure 2. Topology of a road network

In the next sections some special aspects of the algorithm related to the requirements of our application are described.

### 2.3 Image energy

In this paper the image energy is generally defined by a weighted sum of three components derived from ALS data:

$$E_{img} = a \cdot E_I + b \cdot E_{DSM} + c \cdot E_{Var} \tag{9}$$

where $E_I$ = energy from intensity image
$E_{DSM}$ = energy from DSM
$E_{Var}$ = energy from surface roughness
a, b, c = weights.

Initially, the unfiltered height as well as the intensity information is modelled in a regular grid by means of the common interpolation algorithm kriging in a pre-processing step (Cressie, 1990). The intensity image is smoothed by a median filter in order to remove outliers as well as decrease the noise while preserving the road edges. Intensity values of the ALS data represent the reflectance properties of the illuminated objects according to the wavelength of the emitted beam (near

infrared). Road surfaces such as asphalt generally appear dark due to the high absorption rate (Clode et al., 2007). Therefore, the pre-processed intensity image determines the first part of the image energy forcing the snake to low grey values. However, some other objects such as building roofs show a similar behaviour and disturb the optimization process related to this energy part.

The second image energy term is defined by the DSM. For the adaptation of road networks to the ALS data, which is the main issue of this paper, the unfiltered heights are used in order to preserve information of context objects such as buildings or trees. Generally, in urban areas the road surface is lower than the surrounding areas. However, roads on bridges or embankments disturb this assumption. Usually, the normalised DSM (nDSM) should be used in order to remove the influence of the terrain (Weidner & Förstner, 1995). The chosen test area in Schleswig-Holstein is very flat. Thus, the difference between the DSM and nDSM is not considered in the examples.

Assuming that the resolution of the data is sufficient, a small local variation of the heights indicates a smooth surface, which is to be expected for roads. Therefore, the roughness of the terrain offers another option for being a part of the image energy. For this purpose the standard deviation of the DSM is calculated in window of different sizes. Our experiments have shown that a window size of $13 \times 13$ m$^2$ is sufficient for delineating road surfaces from vegetated areas or border regions to higher objects.

The weights a, b, c of the energy parts in Equation 9 are determined empirically supported by the histograms of the images. Several combinations are illustrated in the results. For the application of the network snakes to road centrelines such a basic definition of energy may be suitable. For the adaptation of road regions more sophisticated pre processing steps such as edge detectors or special data fusion methods are necessary. This fact is beyond the scope of this paper and will be tackled in future research.

### 2.4 End nodes

Due to the arc length minimising effect related to the definition of the internal energy the network snake generally tends to shrink. Especially contour parts ending in nodes with a degree of one suffer from this aspect, since neither the topology nor the image energy can alleviate this behaviour. Strong gradients across the contour direction for the image energy, which are able to counteract, are usually not available because roads are homogeneous both in intensity and height. In the original approach of Butenuth (2008) the x or y coordinate of the end node is fixed at the image border. This approach is sufficient if the desired features are boundaries of adjacent objects. However, in this application roads do have dead ends. Thus, this problem has to be tackled in another manner. A post processing step is carried out after each iteration. The new position of the end nodes is calculated by intersecting a straight line perpendicular to the contour direction containing the end node of the previous iteration and the current contour segment between the end node and its neighbour. This allows the motion of the end node across the contour direction. Additionally, a threshold for the variation in the direction of the contour is defined in order to avoid glancing intersections and automatic changes in the point order.

## 3. EXPERIMENTS

In this section the network snake approach is applied to a ALS data set from Schleswig-Holstein near the village Kellinghusen and roads from ATKIS vector data.

### 3.1 Data

The ALS data set is acquired by the company TopScan during a countywide flight campaign of Schleswig-Holstein between 2005 and 2007. Flying at an altitude of 1000 m the system ALTM 3100 from Optech was used in the first and last echo mode to provide an overall point density of 3-4 points/m$^2$ and a required accuracy of 0.15 m (height) and 0.3 m (position). From the ALS data a grid of 1 m resolution is interpolated. The ATKIS vector data set (road network only) was manually digitized in orthophotos in order to create reliable ground truth. Afterwards the position was shifted by different distances in several directions (in the example used in Figures 3-6: 9 m in x and 9 m in y direction) to simulate the inconsistent ATKIS data base which is used for initialisation in our analysis.

### 3.2 Results

Figures 3 - 5 as well as Table 1 depict the comparison of the initialisation, ground truth and the final position of the network snake in a village region using different definitions of the image energy. The energy optimisation process is performed using the same parameters in any case. The parameter $\beta$ is set to a large value compared to $\alpha$ in order to take into account the straight shape of the roads. The image energy in Figure 3 is calculated from the ALS intensity setting the other weights in Equation 9 to zero. The image was smoothed by means of a 3x3 median filter. Several contour parts do not converge to the desired position. The snake is often caught by local minima caused by building roofs in the vicinity of the streets with similar reflectance properties as road surfaces.

Figure 3. Image energy from intensity values (green: ground truth; blue: initialisation; red: final position)

In Figure 4 a smoothed ALS surface model represents the image energy. The bridge at the top of the image disturbs the final position of the snake, since the road is higher than its surrounding area. Furthermore, the dark (low) regions between

the buildings are often too wide containing garden areas in order to attract the road network to accurate positions.

The image energy in Figure 5 is defined by a combination of intensity and height information exploiting features of two sources. In comparison to the ground truth the network snake converges to a satisfying position.

Figure 4. Image energy from unfiltered ALS heights (green: ground truth; blue: initialisation; red: final position)

Figure 5. Image energy from a combination of intensity and height values (green: ground truth; blue: initialisation; red: final position)

The accuracy values in Table 1 support the interpretation of the visual results. In the second column the mean point to contour distance between the ground truth and the initialisation as well as the final position of the snake for different image energies is illustrated. This distance is used, because the motion of the nodes is mainly caused by an along contour component which is not essential in this application. Thus, the accuracy measure across the contour direction is more significant. In the third column of Table 1 the related standard deviation of the distance is given.

Setting the other weights in Equation 9 to zero single image energies slightly improve the position of the network snake. For example, using the DSM energy only the mean distance is decreased in comparison to the initialisation by about 4m. Although some contour parts correctly delineate the roads, the position of the snake in other areas is even worse than the initialisation. In contrast combined image energies perform better. For instance, the use of a combined equal weighted height and intensity image energy improves this point to contour distance from 9m to 3m. This still large difference is also caused by an incorrect position of the ground truth which does not always exactly delineate the centreline of the road network.

| Image energy | Mean point to line distance [m] | Standard deviation of the distance [m] |
|---|---|---|
| Initialisation | 8.97 | 3.02 |
| Intensity | 6.69 | 5.26 |
| DSM | 4.88 | 4.16 |
| DSM+Intensity | 2.98 | 2.63 |
| DSM+Deviation | 3.10 | 2.41 |
| Intensity+Deviation | 4.92 | 4.72 |
| DSM+Intensity+Deviation | 3.23 | 3.78 |

Table 1. Comparison with ground truth (number of nodes: 790)

Analysis in more rural areas show that the integration of texture features such as the standard deviation of the height is more beneficial in order to distinguish between vegetated and artificial surfaces.

Figure 6 visualises the behaviour of the end nodes with and without additional constraints. Obviously, the length of the dead ends in the example without constraints decreases step by step. In contrast, after the introduced post processing steps the length is preserved for the three illustrated end nodes.

Figure 6. Behaviour of the end nodes (blue: initialisation, red after 15 iterations, white: intermediate), top: without, bottom: with additional constraints

## 4. CONCLUSION

In this paper an active contour approach is applied to the adaptation of a road network to ALS data. Even with a simple definition of the image energy by combining ALS height and intensity information promising results could be achieved. Based on the exploitation of the topology of given initialisation the snake converges to the desired position in comparison to the ground truth. Contour parts connected by nodal points support each other during the optimisation process.
The introduced algorithm offers many possibilities regarding the integration of object knowledge for future research. For example, constraints about the shape of the objects (parallelism of road edges, slope constraints) or relations to other ATKIS objects can be incorporated in the initialisation as well as in additional energy terms. Furthermore, a more sophisticated formulation of suitable image energies concerning different vector objects can improve the applicability of the method.

Additionally, the algorithm can be extended to other DLM objects having a relation to features in ALS data such as rivers. Subsequently, all the adapted objects provide a dense network of shift vectors which can be used in addition to prior accuracy knowledge in order to improve the consistency of the DLM and ALS data.

## ACKNOWLEDGEMENT

This research was supported by the surveying authorities of Lower Saxony “Landesvermessung und Geobasisinformation Niedersachsen (LGN)” and of Schleswig-Holstein “Landesvermessungsamt Schleswig-Holstein”. We also express our gratitude to the mentioned surveying authorities for providing the data.

## REFERENCES

Alharthy, A., Bethel, J., 2003. Automated road extraction from Lidar data, *Proc. ASPRS Annual Conference, Anchorage, Alaska,* unpaginated CD-Rom.

Blake, A. and Isard, M., 1998. Active contours. *Springer, Berlin Heidelberg New York*, 351 p.

Borkowski, A., 2004. Modellierung von Oberflächen mit Diskontinuitäten. *Habilitation*, TU Dresden, Germany, 91p.

Burghardt, D. and Meier, S., 1997. Cartographic displacement using the snake concept. In: Förstner, Plümer (eds.), *Semantic modeling for the acquisition of topographic information from images and maps*, Basel, Birkhäuser Verlag, pp. 59-71.

Butenuth, M., 2008. Network snakes. PhD Thesis, University of Hannover, DGK-C 620.

Caselles, V., Kimmel, R. and Sapiro, G., 1997. Geodesic active contours. *International J. Computer Vision* 22(1), pp. 61-79.

Clode, S., Rottensteiner, F., Kootsookos, P, Zeiniker, E., 2007. Detection and vectorization of roads from Lidar data, *PE & RS* 73(5*)*, pp. 517-536.

Cohen, L. D. and Cohen, I., 1993. Finite element methods for active contour models and balloons for 2-D and 3-D images, *IEEE TPAMI* 15(11), pp. 1131-1147

Cressie, N. A. C., 1990. The origins of Kriging, *Mathematical Geology* 22, pp. 239-252.

Kass, M, Witkin, A, Terzopoulos, D., 1988. Snakes: active contour models. *International J. Computer Vision* 1(4), pp. 321-331.

Kerschner, M., 2001: Seamline detection in colour orthoimage mosaicking by use of twin snakes, *ISPRS J. Photogr. & Rem. Sens.* 56(1), pp. 53-64.

Koch, A., 2006. Semantische Integration von zweidimensionalen GIS-Daten und Digitalen Geländemodellen. PhD Thesis, University of Hannover, DGK-C 601.

Laptev, I., Mayer, H., Lindeberg, T., Eckstein, W., Steger, C. and Baumgartner, A., 2000. Automatic extraction of roads from aerial images based on scale space and snakes, *Machine Vision and Applications* 12, pp. 23-31.

Lenk, U., 2001. 2.5D-GIS und Geobasisdaten - Integration von Höheninformation und Digitalen Situationsmodellen. PhD Thesis, University of Hannover, DGK-C 546.

Malladi, R., Sethian, J. A. and Vemuri, B. C., 1995. Shape modeling with front propagation: A level set approach, *IEEE TPAMI* 17(2), pp. 158-175.

McInerney, T. and Terzopoulos, D., 1995. Topologically adaptable snakes. *Proc. International Conference on Computer Vision*, pp 840-845.

Oude Elberink, S., Vosselman, G., 2006: Adding the third dimension to a topographic database using airborne laserscanning, *IntArchPhRS* XXXVI/3, pp. 92-97.

Pilouk, M., 1996. Integrated modelling for 3D GIS, PhD Thesis., Enschede, The Netherlands, *ITC Publication Series No. 40*.

Rieger, W. Kerschner, M., Reiter, T., Rottensteiner, F., 1999. Roads and buildings from laser scanner data within a forest enterprise, *IntArchPhRS* XXXII / 3-W14, pp. 185-191.

Rousseaux, F., Bonin, O., 2003. Towards a coherent integration of 2D linear data into a DTM, *Proc. 21st International Cartographic Conference (ICC).* pp. 1936-1942.

Weibel, R., 1993. On the integration of digital terrain and surface modeling into geographic information systems, *Proc. 11th International Symposium on Computer Assisted Cartography (AUTOCARTO 11)*, pp. 257-266.

Weidner, U. and Förstner, W. 1995. Towards automatic building reconstruction from high resolution digital elevation models, *ISPRS J. Photogr. & Rem. Sens.* 50(4), pp. 38–49.

Xu, C, Prince, J.L., 1997: Gradient Vector Flow: A new external force for snakes, *Proc. IEEE Conference on Computer Vision and Pattern Recognition*, pp. 66-71.

Zhu, P., Lu, Z., Chen, X., Honda, K., Eiumnoh, A., 2004: Extraction of city roads through shadow path reconstruction using laser scanning, *PE & RS* 70 (12), *pp. 1433-1440.*